Fusion Technology

ISSN: 0748-1896 (Print) (Online) Journal homepage: http://www.tandfonline.com/loi/ufst19

An Adaptive Plasma Density Controller at Joint European Torus

H. E. O. Brelén

To cite this article: H. E. O. Brelén (1995) An Adaptive Plasma Density Controller at Joint European Torus, Fusion Technology, 27:2, 162-170, DOI: 10.13182/FST95-A30372

To link to this article: https://doi.org/10.13182/FST95-A30372

Published online: 09 May 2017.

AN ADAPTIVE PLASMA DENSITY CONTROLLER AT JOINT EUROPEAN TORUS

INSTRUMENTATION AND CONTROL

KEYWORDS: *plasma density, plasma density control, adaptive control*

H. E. O. BRELÉN *JET Joint Undertaking*
Abingdon, Oxon OX14 3EA, England

Received May 31, 1994
Accepted for Publication September 19, 1994

An adaptive controller is proposed to replace the current conventional controller in the plasma density feedback system at Joint European Torus (JET). Changing plant dynamics calls for matching retuning of the controller to retain the required performance of the control system. This controller tuning must now be done manually. In the adaptive controller, the retuning process is automated and runs in parallel with the control function. The plant is analyzed, the components of the proposed controller are designed to suit prescribed performance, and the result is illustrated in simulations.

INTRODUCTION

The plasma particle density is one of the most important variables in tokamak fusion activities. For this reason, considerable efforts are being made to keep this variable under control to some degree of accuracy. In most experimental devices of this kind, plasma particle density is controlled by a simple automatic system that adjusts the gas inlet to the plasma so that the difference between the reference and measured plasma density is minimized, as indicated in Fig. 1.

At the Joint European Torus (JET), the plasma density, or more accurately the electron density, is normally measured by a laser interferometer with a vertical line of sight through the torus. The measured density signal is validated by comparison with other diagnostics that produce estimates of the plasma density. If the interferometer signal is found to be unreliable in this validation, it will be replaced automatically with the signal from another diagnostic, for instance, bremsstrahlung. The gas introduction system incorporates a multitude of gas reservoirs for different types of gas, valves, and inlets that can be selected as appropriate for the experiments. At present, the controller is of the classical proportional-integral-derivative type, implemented in a front-end microprocessor.[1,2]

Reconfigurations in the gas introduction system affect the dynamic properties of the feedback loop and hence its control performance. These changes can be compensated for by retuning the controller on the basis of experience of the way those reconfigurations influence the control system.

However, changing properties in the plasma and in its interaction with the vacuum vessel wall also affects the performance of the control loop. The steady-state and dynamic density responses to a given gas inflow differ in character over time, and these changes are much more difficult to compensate for because in practice they are unpredictable and vary during each experiment. In unfortunate cases, these character fluctuations can even make the system unstable.

To eliminate the need for the sometimes impossible task of manual retuning, an adaptive controller is proposed to replace the current controller. Such a controller will automatically adapt to the ever-changing plant dynamics in an effort to maintain prescribed control performance.

REQUIREMENTS

An improved plasma density controller should meet the following performance requirements:

1. The settling time to within 1% deviation from the steady-state value of the controlled signal should be 1.5 to 2 s following a stepwise change in the reference signal.

2. The overshoot following a stepwise change in the reference signal should be no more than 5% above the steady-state value of the controlled signal.

3. No steady-state error to step is allowed.

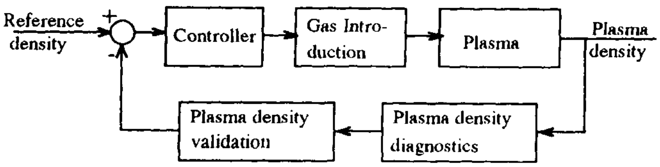

Fig. 1. Schematic representation of the existing plasma density control system.

4. Steady-state deviation in plasma density due to disturbance should be at least a factor of 20 less than that of an uncontrolled system.

5. Sudden changes over the whole expected plant parameter range must not cause any instability of the system, and 20-s recovery time to these performance figures is acceptable.

SUGGESTED SYSTEM

Two main problems must be considered:

1. In view of the dynamics of the plant, the required performance of the controlled system is difficult to achieve with the current type of controller.

2. The dynamic properties of the plant under control vary with time.

Provided an accurate model of the plant is known and as long as the actuation does not cause any saturation, a controller of sufficiently high order and degree of freedom in the design process makes next-to-arbitrary control performances achievable. The controller must be tuned in relation to the plant it is controlling. If the dynamic character of the plant is changing, the controller tuning must be updated accordingly to maintain the control performance.

The parameter set Θ, describing the plant characteristics, which is required for the calculation of the controller parameters, is obtained by an identifier. The identification is done on synchronized samples of the plant input signal U and its output signal Y. The plant parameters are identified, and the controller parameters are recalculated at each sampling occasion, which keeps the controller adapted to ongoing plant changes.

Two control loops can be distinguished in the controlled system, as shown in Fig. 2. One loop handles the parameters in the adaptation process, and one loop handles the states in the control process.

PLANT MODEL

As mentioned earlier, the design of the controller depends on a model of the plant to be controlled. The absolute values of the model parameters are not important here (the adaptive process is expected to take care of them), but the order of the model, nonlinearities, parameter variations, and disturbances are crucial for the design.

The basic process in this model is the circulation of particles into and out of the plasma. A global particle balance study[3,4] leads to the following equation:

$$\frac{dN_p}{dt} = -\frac{N_p}{\tau_p} + \frac{f}{1-r(1-f)} \times \left[r\frac{N_p}{\tau_p} + \frac{N_w}{\tau_w} + r(1-f_e)\Phi\right] + f_e\Phi \ , \quad (1)$$

where

N_p = particle inventory in the plasma

τ_p = global plasma particle confinement time, typically 0.2 s

N_w = particle inventory in the vessel wall

τ_w = wall particle confinement time, typically 10 s to 10 min

r = reflection coefficient, normally between 0.1 and 0.5

f = fueling efficiency of the recycled particles, typically 0.1 to 0.5

Φ = external flow of particles

f_e = fueling efficiency for the external flow, again typically 0.1 to 0.5.

The plasma receives particles not only from the external flow but also from releases from the vessel wall. At the same time, particles are lost from the plasma, most of which are absorbed in the wall. A similar particle balance equation can be written for the vessel wall, which completes the global particle balance in the vessel:

$$\frac{dN_w}{dt} = -\frac{N_w}{\tau_w} + \frac{1-r}{1-r(1-f)} \times \left[\frac{N_p}{\tau_p} + (1-f)\frac{N_w}{\tau_w} + (1-f_e)\Phi\right] \ . \quad (2)$$

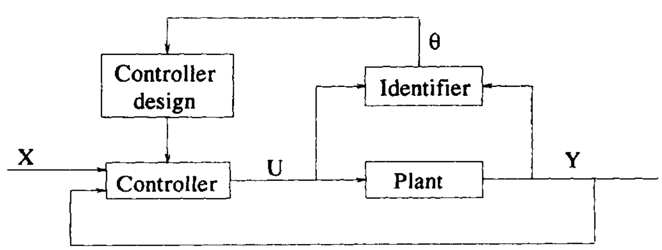

Fig. 2. Structure of adaptively controlled system.

The accumulated external inflow of particles is shared between the wall and plasma inventories during transients, because of changes in inflow or disturbances, as well as in equilibrium states. Combining Eqs. (1) and (2) by eliminating N_w and then rewriting the result in transfer function form gives the following equation:

$$\frac{N_p(s)}{\Phi(s)} = \frac{K_p(s + z_1)}{s(s + p_1)} \ , \tag{3}$$

where the physical parameters are summarized in the model parameters as follows:

$$K_p = \frac{fr + f_e(1 - r)}{1 - r(1 - f)} \ ,$$

$$z_1 = \frac{f}{\tau_w[fr + f_e(1 - r)]} \ ,$$

and

$$p_1 = \frac{\tau_w(1 - r) + \tau_p f}{\tau_p \tau_w[1 - r(1 - f)]} \ . \tag{4}$$

Expected variations in physical parameters, as indicated earlier, will obviously affect the gain and the location of the transfer function zero and pole. The pole will be found at approximately $-1/\tau_p$, provided τ_w is much larger than τ_p and the fueling efficiencies and reflection coefficient are within the expected ranges. Under the same assumptions, the location of the zero will be in the vicinity of $-1/\tau_w$, and because the variation of τ_w is expected to be large, the corresponding movement of the zero will have a strong effect. In one extreme case in which the value of τ_w nears that of τ_p, the zero approaches the pole at $-p_1$ and gradually eliminates its effect, hence turning the process into an integrator. In the other extreme with large τ_w values, corresponding to a heavily absorbent wall, the zero will move toward the integrator pole at the origin, changing the dynamic character of the process to that of an exponential delay with time constant τ_p.

This effect is in line with what has been observed in experiments at JET, particularly in open-loop step response tests.[1] These tests also revealed some dynamics from the gas introduction system, identified here as an exponential delay with time constant $1/p_2 = 1.2$ s and a transport delay of $L = 0.2$ s. Because the system has a serial structure, the total transfer function from gas introduction request U to measured plasma density Y is written as follows:

$$\frac{Y(s)}{U(s)} = \frac{K[\exp(-sL)]\,(s + z_1)}{s(s + p_1)(s + p_2)} \ , \tag{5}$$

where it is assumed that the measured density Y is proportional to the plasma particle inventory N_p. Variations in the density profile will also affect this proportionality and are considered here as another parameter variation. A few step responses for this model are shown in Fig. 3, for different values of τ_w, highlighting the effect of the moving transfer function zero. Varying τ_w from 10 to 640 s moves the zero from -0.4 to -0.006, while the pole moves from -5.03 to -5.0 and the Bode gain $K z_1/p_1 p_2$ varies from 22 to 0.34 (K is given the empirical value 234 interferometer fringe/$\mathrm{V \cdot s^2}$).

A great variety of conceivable parameter variations must be considered. However, those illustrated in Fig. 3 are believed to be among the worst that can be expected and, as such, are taken as the basis for the controller design. Furthermore, although physically impossible, the instantaneous change in τ_w from one extreme to the other is considered as a test case scenario.

ANALYSIS OF REQUIREMENTS

As with the plant itself, the poles and zeroes of the closed-loop system reflect its dynamic properties. When suitable controller transfer functions are selected, the controlled system's poles can be located at positions that correspond to the desired performance. Thus, given the requirements in time format, it is now a matter of translating these requirements to controlled system pole locations.

Among the poles and zeroes of the closed-loop system, some will be more dominant than others and will in practice determine the dynamic character of the system. If a complex pole pair with a damping ratio of 0.7 is made to dominate, the system will exhibit the permitted 5% overshoot. The reason for aiming for the borderline case is to keep the rise time short. The dominant pole pair is also designed to have an undamped natural frequency of 5 rad/s to satisfy the settling time requirement.

Because the controller is to be implemented in a front-end computer working in discrete time with sampled data, this discussion is now continued in the discrete time domain. First, the sampling rate must be determined. Because the system bandwidth is just above the previously specified resonance frequency, a 0.2-s sampling interval is considered adequate. This interval gives the positions for the dominant poles of the controlled system transfer function as $0.4 \pm 0.3i$ in the z plane. All remaining poles should be made less dominant by locating them at $z \leq 0.3$.

After the sampling interval is determined, the plant model is also converted to the z domain. It will be used in simulations to follow and later to provide the "true" parameter values for the black box identification. A discrete time-pulse transfer function for the plant model with $\tau_w = 10$ s and the chosen sampling rate is as follows:

$$\frac{Y(z)}{U(z)} = \frac{0.9850z^{-2} - 0.2260z^{-3} - 0.6339z^{-4}}{1 - 2.2123z^{-1} + 1.5219z^{-2} - 0.3096z^{-3}} \ , \tag{6}$$

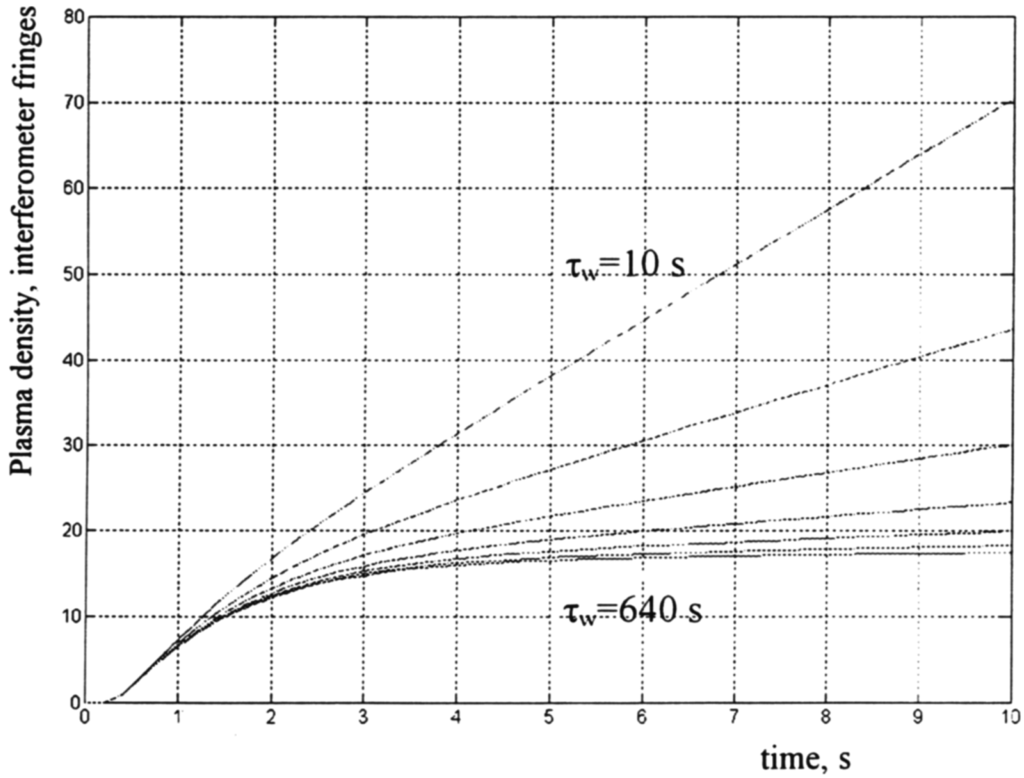

Fig. 3. Step responses from the plant model for $\tau_w = 10, 20, 40, \ldots, 640$ s; $\tau_p = 0.2$; $f = 0.2$; $f_e = 0.3$; $r = 0.3$.

where the transport delay, which is one sampling period, is taken into account.

CONTROLLER

A controller with the following control law is now introduced[5–7]:

$$R \cdot u = T \cdot x - S \cdot y \ , \tag{7}$$

in which R, T, and S are polynomials of the discrete time shift operator z. Several restrictions, due to causality requirements, on the degree of these polynomials exist, but sufficient freedom still remains for the design of the controller.

The structure of the controlled system is shown in Fig. 4 for which the (closed-loop) transfer function is

$$\frac{\boldsymbol{y}}{\boldsymbol{x}} = \frac{\boldsymbol{T} \cdot \boldsymbol{B}}{\boldsymbol{A} \cdot \boldsymbol{R} + \boldsymbol{S} \cdot \boldsymbol{B}} \ , \tag{8}$$

where B and A are the numerator and denominator polynomials in the plant transfer function. The R and S polynomials are chosen to be of third order, and because the plant is of order four, the total system is of order seven. The controlled system has seven poles of which the most dominant two are required to be at $z = 0.4 \pm 0.3i$ and the rest are at $z \leq 0.3$. Given B and A, it is now possible to find R and S by identifying the coefficients in the $AR + BS$ polynomial with those in a seventh-order polynomial that is made to have the required zeroes. The result can be summarized in the following matrix equation:

$$\begin{bmatrix} \boldsymbol{r} \\ \boldsymbol{s} \end{bmatrix} = [ab]^{-1} \cdot \begin{bmatrix} a_{m1} - a_1 \\ a_{m2} - a_2 \\ a_{m3} - a_3 \\ a_{m4} \\ \vdots \end{bmatrix} \ , \tag{9}$$

where

$\boldsymbol{r}, \boldsymbol{s}$ = vectors containing the coefficients for R and S

$[ab]$ = Sylvester matrix containing the plant parameters

$a_{m1} \ldots a_{m7}$ = coefficients in the polynomial with the required zeros

$a_1 \ldots a_3$ = coefficients in the plant polynomial A.

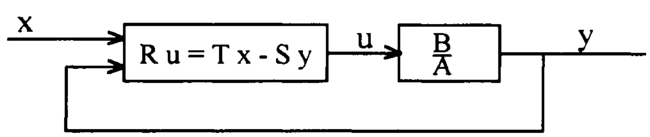

Fig. 4. Flow chart of controlled system.

Before this calculation is completed, it should be noted that the controlled system has zeroes in common with the plant. In many cases, this situation causes no concern, but the zero that approaches the origin (or $z = 1$ in the z plane) will have a very strong effect on the system response. Its effect is made worse by the fact that, unlike the open-loop transfer function, the controlled system does not have an integrator pole to reduce it. Overshoots caused by this zero can be several times larger than the steady-state level. When one of the poles of the controlled system coincides with this zero (that is, the zero in B is also a zero in $AR + BS$), its effect is cancelled, and the intended system performance should be seen. Figure 5 illustrates the effect of cancelling the plant zero in the relatively mild case in which $\tau_w =$ 10 s.

As already discussed, the situation is further complicated by the fact that the plant zero and poles move because of changing plant parameters. To maintain the performance of the system, its poles must be kept in the required positions, including the one that cancels the zero; therefore, the calculation of the coefficients of the controller polynomials R and S must be repeated at each sampling occasion, with the latest A and B polynomials. Up-to-date values of these plant parameters are obtained by an identifier.

If the identification process finds that the plant zero is outside the unit circle, which has been noted in identifications based on real data, then for stability reasons, no attempt will be made to cancel it with a pole. Furthermore, if the plant zero is inside the unit circle but is fast enough, say $|z| \leq 0.3$, then again, no attempt will be made to cancel its effect. In both cases, the pole used for cancelling will be put among the other ones at $z \leq 0.3$.

Finally, polynomial T is also chosen to be of third order, introducing three additional zeroes in the controlled system's transfer function. These zeroes should also be fairly "fast," $|z| \leq 0.3$, and in fact, they can be placed on top of the poles already located in this area. One purpose of polynomial T is to reduce the difference between the number of poles and zeroes in the closed-loop system, thus avoiding unnecessary time-step delays. With the chosen order, this difference is made the same as in the original plant.

LEAST-SQUARE IDENTIFIER

The identifier algorithm chosen for this application is the recursive least-square identification.[5–7] It is based on the minimization of the loss function:

$$J(\theta) = \sum_{j=1}^{n} \beta^{n-j}(y_j - \varphi_j^T\theta)^2 \ , \tag{10}$$

where

y = plant output

$\varphi^T\theta$ = identifier's estimate of the plant output calculated from the parameter vector $\boldsymbol{\theta}$ and the measurement vector $\boldsymbol{\varphi}$

β = weight factor for which the value is to be chosen between 0 and 1.

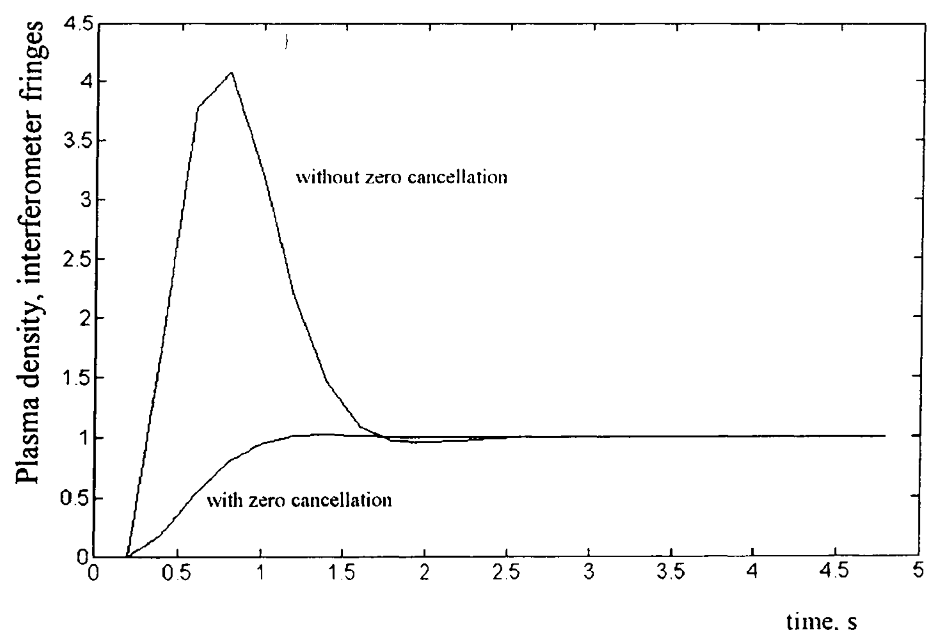

Fig. 5. Simulated unit step responses from a controlled system with and without zero cancellation; $\tau_w = 10$, $\tau_p = 0.2$, $f_e = 0.3$, $f = 0.2$, and $r = 0.3$. (Sampled points are joined with straight lines.)

The most recent estimation error has the greatest influence on the loss function, while the influence of the historic values declines exponentially. This will make the identifier forget old errors and attempt to follow changes in the plant parameters.

The measurement vector is defined as follows:

$$\varphi_n^T = (y_{n-1} y_{n-2} y_{n-3} u_{n-1} u_{n-2} u_{n-3}) \ . \qquad (11)$$

Ultimately, this equation leads to the following result:

$$\theta_{n+1} = \theta_n + K_{n+1}(y_{n+1} - \varphi_{n+1}^T \theta_n) \ , \qquad (12)$$

where

$$K_{n+1} = \frac{P_n}{\beta} \varphi_{n+1} \left(\frac{1}{1-\beta} + \varphi_{n+1}^T \frac{P_n}{\beta} \varphi_{n+1} \right)^{-1} \qquad (13)$$

and

$$P_{n+1} = \frac{1}{\beta} (I - K_{n+1} \varphi_{n+1}^T) P_n \ . \qquad (14)$$

Note that the parameter vector is updated with a term proportional to the estimation error. The proportionality factor, in turn, depends on the statistical properties of the incoming data and the forgetting factor.

IDENTIFIER ROBUSTNESS

It is essential that the identifier be protected from irrelevant data that would disturb the identification process. For instance, the identifier should be switched off and the parameters should be frozen during the earliest and latest stages of the pulse when the correlation between the valve control signal and the plasma density is expected to be poor. The controller on the other side should always run with at times frozen parameter values.

Expected actions like neutral beam or radiofrequency injection or the launching of pellets, which influence the plasma density without any correlation to the gas valve signal, also threaten to disturb the identification process. Again, the identifier can be protected by stopping it on the basis of *a priori* information about these disturbances. In addition, the identifier can be made robust to meet not only these expected disturbances but also unexpected ones.

An effective way of making the identifier robust is to scale the gain for the estimation error in the parameter updating Eq. (12) with a factor that decreases with increasing estimation error. Reasonable errors are let through with their normal weight, while in the short term, sudden large errors are regarded as irrelevant and ignored. However, if they are persistent, the identifier will ultimately adjust to these values. A new mode may have developed, so this new situation should not be rejected completely.

SIMULATION OF IDENTIFIER

To see how the identifier finds the plant parameters, the plant model given [Eq. (6)] is driven by a square wave with a 10-s period. The model input and output signals are presented in parallel to the identifier for recursive identification. Initially, the parameter vector of the identifier is set to 0, and the plots in Fig. 6 show how the six parameters converge toward steady-state values. The rate of convergence depends on β and the degree of excitation. The simulated case shown is for $\beta = 0.97$.

By the end of this simulation, which lasts 50 s in real time, the parameters have practically stabilized at their true values, as given in Eq. (6). In reality, the parameter vector is never reinitialized to zero. Parameter values identified during one pulse are used as the starting point for the next, making the learning process continuous across the experiments.

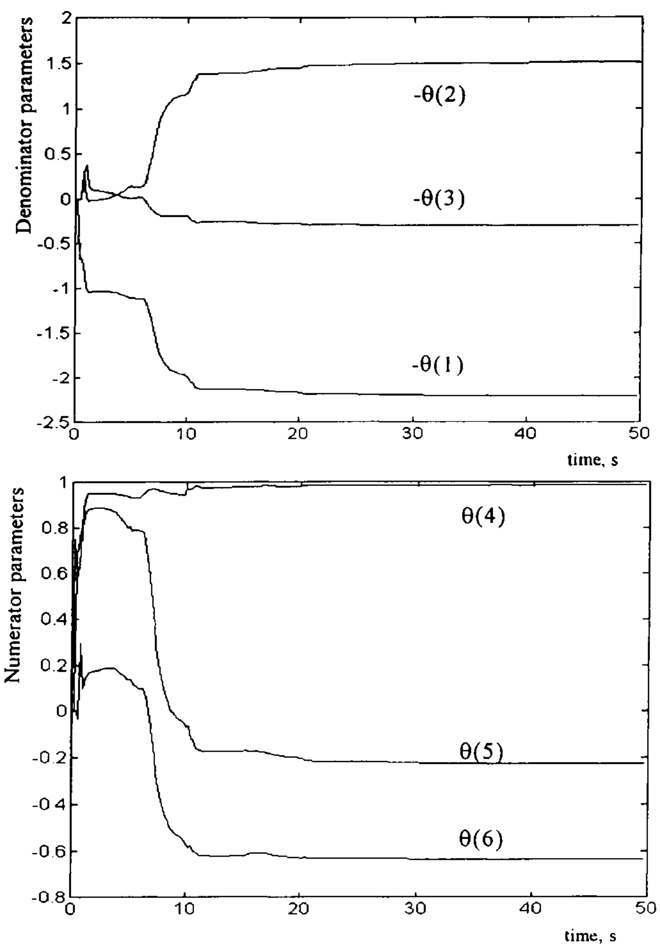

Fig. 6. Transients of identified denominator parameters, top, and numerator parameters, bottom, from zero toward steady state.

TOTAL SYSTEM

All the building blocks are now defined, and the whole system can be assembled as indicated in Fig. 2.

All the functions, identification, updating of controller parameters, and calculation of the control action are executed at every sampling occasion. The sequence of events is as follows:

1. Sample the plasma density signal.

2. Calculate a new identified parameter vector according to Eqs. (12), (13), and (14), provided correlation is expected.

3. Insert the newly identified plant parameter values in Eq. (9) and calculate a new set of controller parameters.

4. Sample the reference signal.

5. Calculate a new control action according to Eq. (7) with the new parameter set and on the basis of the just sampled plasma density signal and the reference signal. Also, previous plasma density values, reference values, and control actions are required for this calculation, so they are stored and permutated for this purpose.

6. Output the control action and wait for next sample occasion.

SIMULATIONS OF TOTAL SYSTEM

Figures 7 and 8 show the results of a simulation of the total system in which the plant time constant τ_w was changed instantaneously from 10 to 640 s, 20 s into the simulation. A square wave switching between plus and minus one and with a time period of 10 s is used as a reference signal (should be regarded as incremental at some arbitrary level). During the simulation, the identifier's β value is set to 0.97.

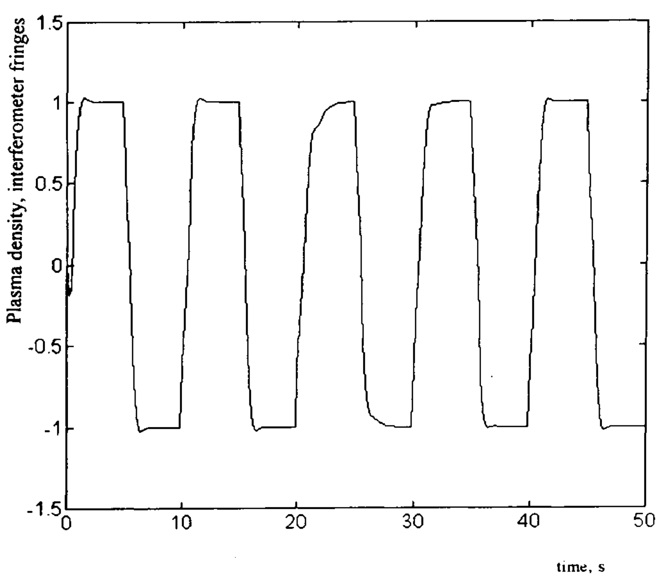

Fig. 7. Simulation of adaptively controlled system with plant parameters changing at 20 s.

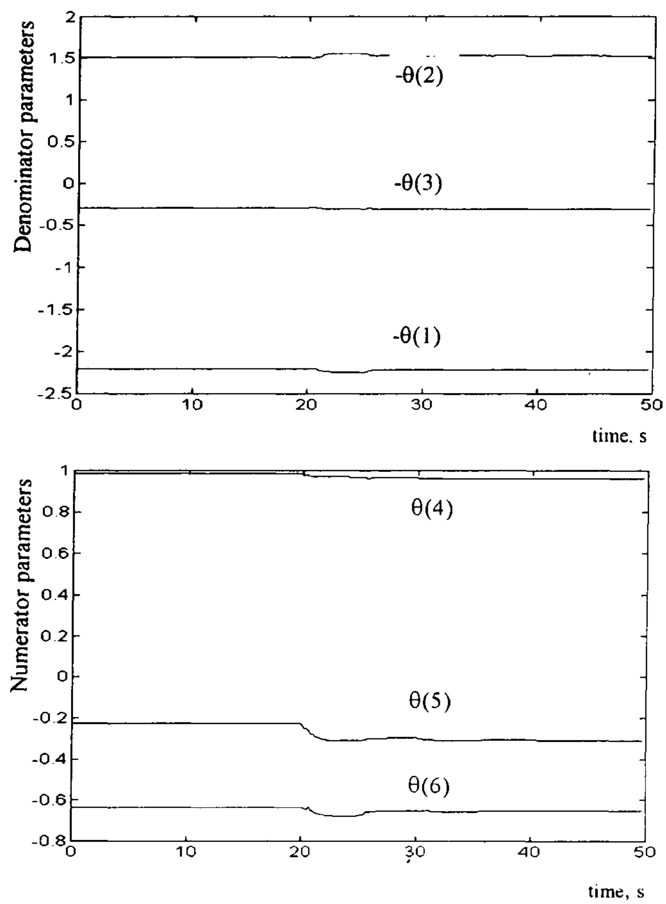

Fig. 8. Identified parameter set as it develops during the simulation.

The jump in plant parameters affects the system for ~15 s after which the performance of the control is restored to an acceptable level. The duration of the learning process is within the specification, and it would have been shorter if the reference signal had had shorter static periods, because the identifier learns from the transients. In the real implementation, the excitation will rely on signals resulting from the control actions.

Because of the learning transients, the closed-loop poles moved during the simulation, as shown in Fig. 9. The change in plant parameters caused the controlled system's poles to make an excursion in the z plane followed by a period of convergence back to their desired locations. The poles stayed well within the unit circle, indicating that the system remained stable during the transition.

STATE DISTURBANCE

Another simulation was made to show the consequence of a step disturbance applied at the plant input.

Without controller action, nearly 20 interferometer fringes were added to the density between 20 and 40 s because of the disturbance. Figure 10 shows that the controller suppresses the disturbance to acceptable levels. Of course, because the disturbance acts on the plant input, it will build up some effect in the plant before the controller becomes aware of it, which explains the transients that occur when the disturbance is applied and taken away.

The robustness of the identifier is crucial here. Without it, a disturbance of this kind puts the identifier on an irrelevant track, and some very poor control in the disturbance counteraction follows.

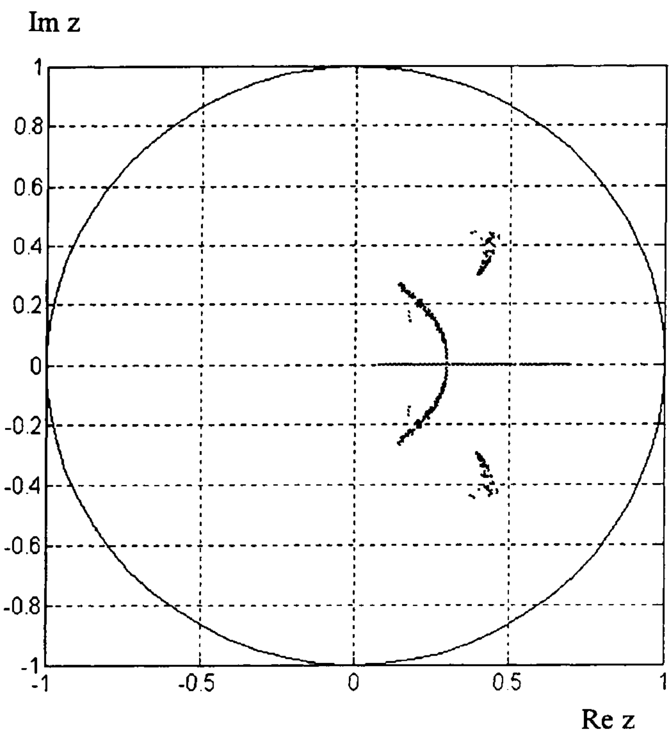

Fig. 9. Locus of closed-loop poles during simulation.

TEST WITH AUTHENTIC DATA

Because the identifier is a measuring device, it can be run off-line with real plant data, provided there is good correlation between the recorded U and Y signals.

For the following tests, data from pulse number 20570 are used. The Y is taken as the validated density, and the U is the control signal actuating the gas valve.

Data are stored with 40-ms sampling intervals, and to obtain the earlier determined sampling interval (0.2 s), every fifth value is used. First, the data are low-pass-filtered by a second-order Butterworth filter with a resonance frequency of 1.25 Hz to reduce the aliasing. The filtered signals are shown in Fig. 11.

The situation in this real case is far from ideal and not as clean as in the simulations. Disturbances and other variations in the plasma density that do not depend on the gas inlet mixed with expected variations will make the identification difficult. In this case, for instance, the plasma density validation decided to switch over to bremsstrahlung measurement at 6 s, causing an unexpected jump in the signals. Also, the start of the pulse as well as its end were turbulent, which contribute negatively to the identification, as can be seen in Fig. 12, because protection or robustness is intentionally not included in this identification. Even so, it is noticeable that the identifier seems to find its way and

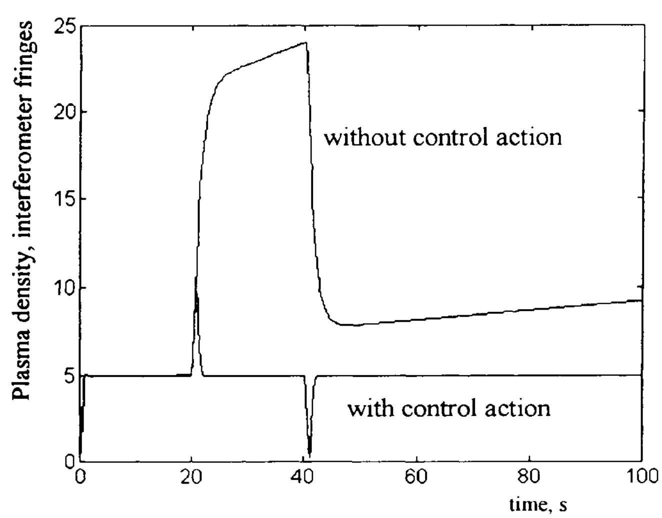

Fig. 10. System response to a disturbance between 20 and 40 s with and without control action.

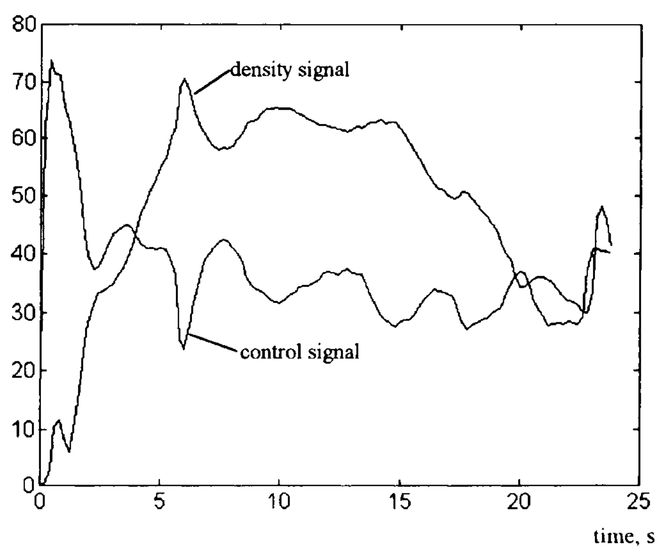

Fig. 11. Plasma density and control signal (magnified ten times) in pulse 20570.

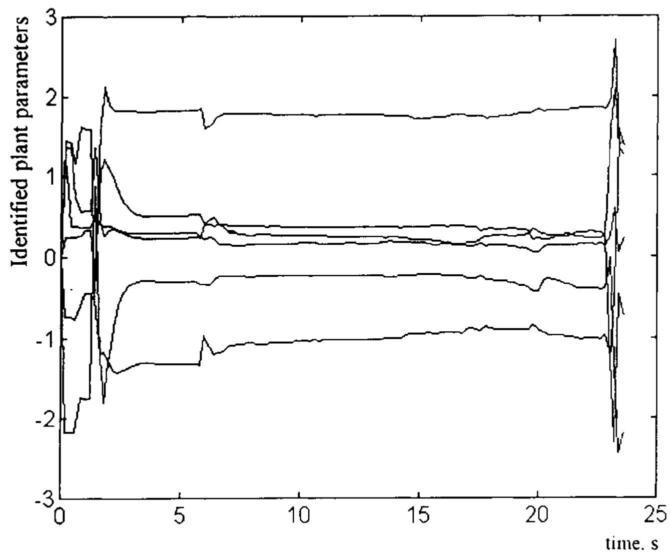

Fig. 12. Time records of identified parameters.

converges to a credible level. It is obvious that robustness is essential, and it should be included in the implementation. Otherwise, it takes many valuable seconds of good data to recover from the start-up transient. Just after the start-up transient, the identified model is even unstable.

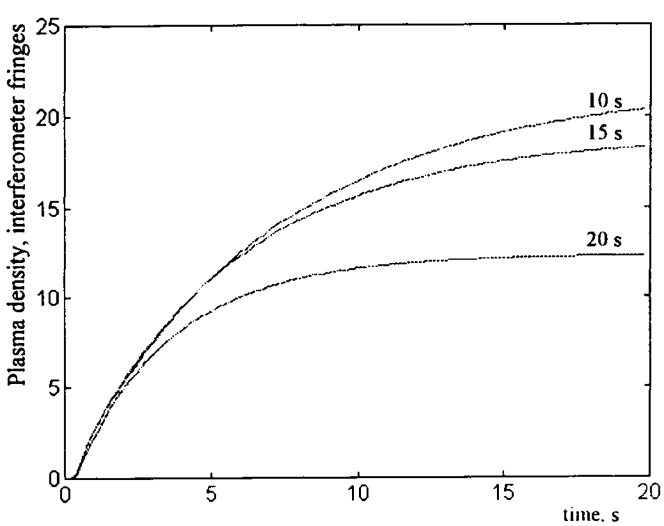

Fig. 13. Unit step responses from model as identified at 10, 15, and 20 s.

The parameter vector identified at 10, 15, and 20 s gives models with step responses as shown in Fig. 13. It is interesting to find that these step responses are similar to what is anticipated. The changing dynamics through the pulse could be explained by an increasing τ_w.

CONCLUSIONS

The adaptive controller proposed here would not only provide improved control performance in the plasma density control system but also alleviate the need for controller retuning due to changes in the plant dynamics. The suggested approach to this control problem seems to be feasible, but an important issue in the implementation will be the robustness of the controller. This factor is particularly important in an experimental environment such as that at JET, where the process to be controlled is run in pulses.

REFERENCES

1. H. E. O. BRELÉN, "Design of Controller for the Plasma Density Feedback System," Internal Report, JET Joint Undertaking (1990).

2. J. HOW et al., "JET Gas Economy with C and Be First Wall and Implication for the Gas Introduction System," *Proc. 16th Symp. Fusion Technology*, London, United Kingdom, September 3-7, 1990, p. 728 (1990).

3. J. K. EHRENBERG et al., "Material Related Aspects of Density Control in JET Plasma Discharges," *J. Nucl. Mater.*, **196-198**, 992 (1992).

4. J. K. EHRENBERG et al., "Plasma Fuelling Experiments in JET and Implications for Future Divertor Operations," *Europhys. Conf. Abs.*, **17C**, Part II, 563.

5. K. J. ÅSTRÖM and B. WITTENMARK, *Adaptive Control*, Addison-Wesley, Reading, Massachusetts (1989).

6. K. J. ÅSTRÖM and B. WITTENMARK, *Computer Controlled Systems: Theory and Design*, Prentice-Hall, Englewood Cliffs, New Jersey (1984).

7. G. F. FRANKLIN, J. D. POWELL, and M. L. WORKMAN, *Digital Control of Dynamic Systems*, 2nd ed., Addison-Wesley, Reading, Massachusetts (1990).

H. E. O. Brelén (MSc, Chalmers University of Technology, Gothenburg, Sweden, 1970) is currently computer group leader at Joint European Torus (JET). He is particularly interested in automatic control applications and previously developed automatic control systems for driverless buses and adaptive control systems for industrial manufacturing processes. He has also taken part in the development of early warning systems for the nuclear power industry.